Translational predictions of phase 2a first-in-patient efficacy studies for antituberculosis drugs

Jacqueline P. Ernest [1,3], Janice Jia Ni Goh [1,3], Natasha Strydom [1,3], Qianwen Wang [1,3], Rob C. van Wijk [1,3], Nan Zhang [1,3], Amelia Deitchman [1], Eric Nuermberger [2] and Rada M. Savic [1]

[1]Department of Bioengineering and Therapeutic Sciences, University of California, San Francisco, San Francisco, CA, USA. [2]Center for Tuberculosis Research, Department of Medicine, Johns Hopkins University School of Medicine, Baltimore, MA, USA. [3]Shared authorship ordered alphabetically.

Corresponding author: Rada M. Savic (rada.savic@ucsf.edu)

Shareable abstract (@ERSpublications)
A translational pharmacology platform to predict early bactericidal activity https://bit.ly/3NoO89J

Cite this article as: Ernest JP, Goh JJN, Strydom N, *et al*. Translational predictions of phase 2a first-in-patient efficacy studies for antituberculosis drugs. *Eur Respir J* 2023; 62: 2300165 [DOI: 10.1183/13993003.00165-2023].

This article has an editorial commentary: https://doi.org/10.1183/13993003.01108-2023

Received: 25 Jan 2023
Accepted: 2 June 2023

Abstract

Background: Phase 2a trials in tuberculosis typically use early bactericidal activity (EBA), the decline in sputum CFU over 14 days, as the primary end-point for testing the efficacy of drugs as monotherapy. However, the cost of phase 2a trials can range from USD 7 million to USD 19.6 million on average, while >30% of drugs fail to progress to phase 3. Better utilising pre-clinical data to predict and prioritise the most likely drugs to succeed will thus help to accelerate drug development and reduce costs. We aim to predict clinical EBA using pre-clinical *in vivo* pharmacokinetic (PK)-pharmacodynamic (PD) data and a model-based translational pharmacology approach.

Methods and findings: First, mouse PK, PD and clinical PK models were compiled. Second, mouse PK-PD models were built to derive an exposure–response relationship. Third, translational prediction of clinical EBA studies was performed using mouse PK-PD relationships and informed by clinical PK models and species-specific protein binding. Presence or absence of clinical efficacy was accurately predicted from the mouse model. Predicted daily decreases of CFU in the first 2 days of treatment and between day 2 and day 14 were consistent with clinical observations.

Conclusion: This platform provides an innovative solution to inform or even replace phase 2a EBA trials, to bridge the gap between mouse efficacy studies and phase 2b and phase 3 trials, and to substantially accelerate drug development.

Introduction

Mycobacterium tuberculosis remains one of the deadliest infectious agents globally. Tuberculosis (TB) drug discovery and development activity has increased emphasis on shorter, more universal regimens to treat all TB cases independent of resistance status [1]. However, with an increasing number of new drugs and limited resources for clinical trials, further innovation of drug development is imperative to identify effective drugs and regimens more efficiently and with higher confidence [1]. A phase 2a early bactericidal activity (EBA) study is typically the first clinical evaluation of novel anti-TB drug efficacy, with the primary purpose of detecting the presence and magnitude of EBA and informing possible dose–response relationships [2]. However, the cost of phase 2a trials can range from USD 7 million to USD 19.6 million on average, while >30% of drugs fail to progress to phase 3 [3]. This highlights the challenges inherent in translating results in pre-clinical models such as *in vivo* mouse models or *in vitro* hollow-fibre systems, into successful clinical end-points and outcomes. United States Food and Drug Administration guidance for industry on drug development for pulmonary TB states that appropriate animal models can serve as an important bridge between the identification of *in vitro* antimycobacterial effects of an investigational drug and the initiation of clinical trials [4]. However, traditional translation of findings from pre-clinical *in vivo* models, by pharmacokinetic (PK) modelling and allometric scaling to identify the dosing regimen in humans that best matches the efficacious drug exposure in animals is insufficient, as it only covers

exposure, but not response. Mechanistic mouse-to-human PK-pharmacodynamic (PD) models that describe the bacterial kill and PK-PD relationships are better at predicting clinical results, including the results of late-stage trials [5]. Therefore, our objective is to establish a relevant and robust model-based translational platform that can reliably link pre-clinical to clinical drug development and predict early efficacy trials for anti-TB drugs across different compound classes (figure 1). We compiled a comprehensive pre-clinical and clinical database of PK, PD and baseline bacterial growth data for 10 drugs. The drugs used to develop and validate our proposed platform consisted of a bacteriostatic antibiotic, namely ethambutol (EMB); five bactericidal antibiotics, namely isoniazid (INH), delamanid (DLM), pretomanid (PMD), linezolid (LZD), and moxifloxacin (MXF); and four sterilising antibiotics namely rifampin (RIF), rifapentine (RPT), pyrazinamide (PZA) and bedaquiline (BDQ). The translational platform in the present study intends to increase the accuracy of pre-clinical to clinical translation by enabling quantitative prediction of clinical studies from pre-clinical outputs and serves as a foundation for model-informed TB drug discovery and development.

Methods

Drug dataset for model building and validation

To build our model and evaluate its predictive accuracy for clinical EBA, 10 first- and second-line anti-TB drugs (BDQ, DLM, EMB, INH, LZD, MXF, PMD, PZA, RIF, RPT) were selected, for which mouse PK, mouse PD, human population PK models and human clinical EBA data were available.

Data required to assess pre-clinical drug efficacy

A large database of PK and PD data in mice for 10 TB drugs with clinical EBA data was collected (figure 2, supplementary table S1). Most experiments were performed at Johns Hopkins University (JHU; Baltimore, MD, USA), with the exception of DLM, for which PK data came both from JHU as well as from literature for one dose level [6]; EMB, for which PK data came from literature [7]; and LZD, which had data from TB Alliance (New York, NY, USA). PK experiments in BALB/c mice were dose-ranging (between two and 10 dose levels), single or multiple oral dosing for up to 8 weeks, with 29–238 observations of plasma concentration per drug. PD experiments in BALB/c mice infected through aerosol delivery were dose-ranging (between two and 15 dose levels), with treatment durations of 21–70 days, and 55–252 observations of lung CFU counts per drug. Lung CFU counts were measured by plating lung homogenates at designated time points. In the case where DLM mouse PK data showed the unexpected trend of a double peak with a single oral dose (figure 2a), we confirmed the trend with the data provider, JHU.

Mouse PK-PD model development

An integrated mouse PK-PD model, involving a PK model to describe drug exposure, a bacterial dynamics model to account for the mouse immune system and a PD model describing the combined effect of bacterial dynamics and drug effect was developed for each drug. PK data were described using one- or two-compartment models with first order absorption with or without delay, and saturable elimination when necessary. Bacterial growth dynamics without treatment were described using our previously published baseline model (supplementary equation S1) [8]. The baseline model captures the decreased rate of growth over time and attributes the decline to time- and bacteria-dependent immune control over the infection. The drug effect, measured as the $\log_{10}$ CFU drop independent of the immune effect over time, was incorporated using a (sigmoidal) E_{max} (maximal level of drug effect) relationship (supplementary equation S2). A delay effect (K_{delay}) was tested where appropriate to mouse PK-PD models to establish an indirect relationship between plasma drug concentrations and drug effect at the site of action (supplementary equations S3 and S4). Detailed model development and model diagnostics can be found in the supplementary material.

Prediction of the clinical EBA

The PK-PD relationship quantified in mice was used to predict the clinical EBA. Drug concentrations in humans were simulated based on clinical population PK models (supplementary table S1) to drive the concentration–effect relationship in the clinical predictions. Where clinical population PK models were unavailable, allometric scaling from mouse PK model parameters was used [9]. Protein binding ratios between humans and mice ($f_{u,human/mouse}$) were used to convert unbound plasma drug concentrations from human to mouse to translate the mouse PK-PD relationships (supplementary table S1) [10–16].

Clinical predictions for 10 drugs were simulated, with 14 unique studies at several dose levels used for validation by graphically overlaying simulated EBA from pre-clinical models with observed EBA from clinical trials. Predictions were done by simulating CFU decline in 1000 virtual patients treated with the same dose as reported in the clinical EBA study. The baseline (day 0) sputum values used were derived

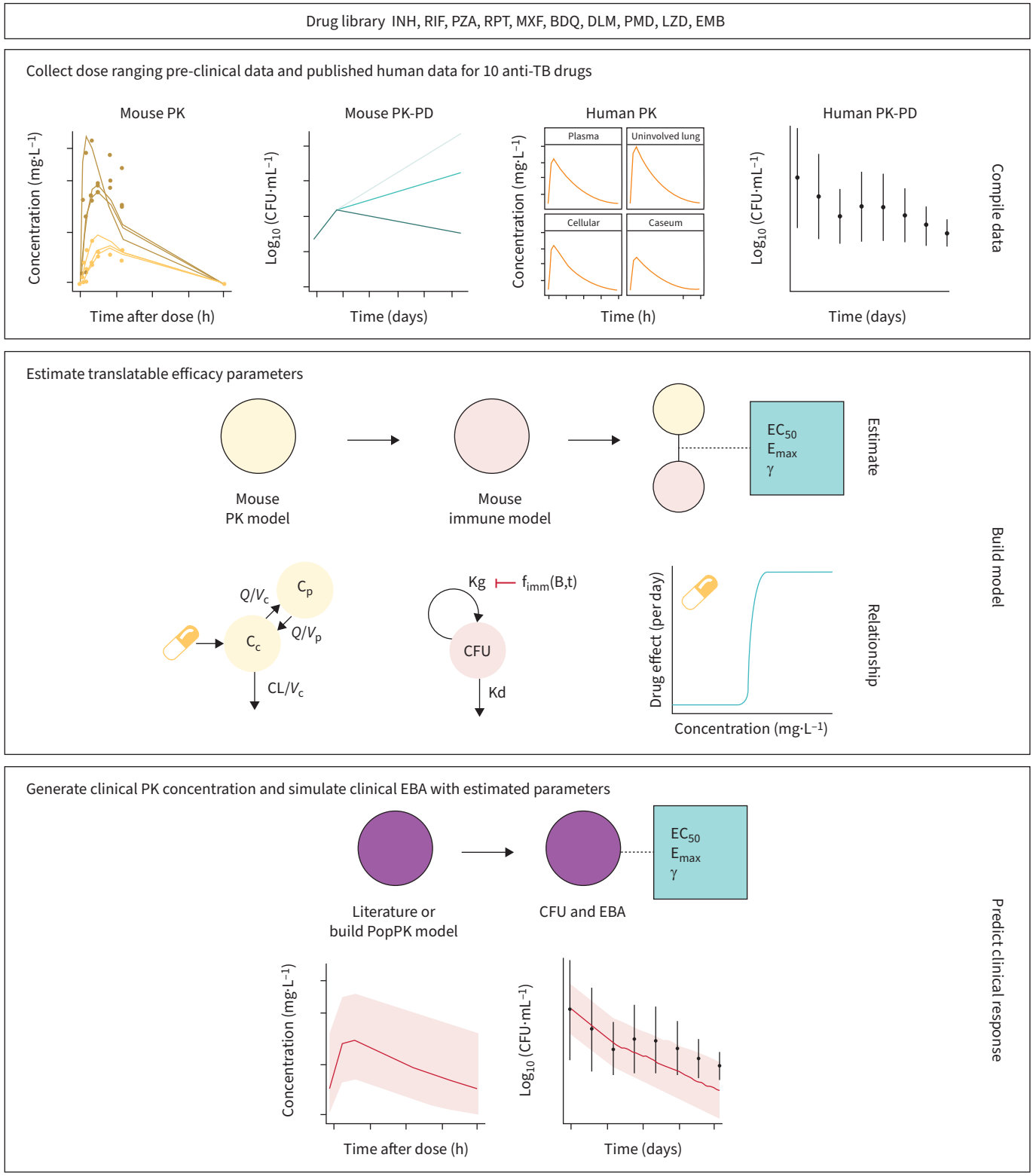

FIGURE 1 The translational pharmacology approach to predicting early bactericidal activity (EBA) in patients. Components necessary for translation include mouse pharmacokinetics (PK)-pharmacodynamics (PD) and clinical PK (actual or scaled). The estimated relationship between drug concentration and bacterial kill is assumed to be portable after correction for protein binding and integrated with clinical PK. Using baseline bacterial burden from previous EBA trials as initial conditions, the EBA is simulated with the translational model. INH: isoniazid; RIF: rifampin; PZA: pyrazinamide; RPT: rifapentine; MXF: moxifloxacin; BDQ: bedaquiline; DLM: delamanid; PMD: pretomanid; LZD: linezolid; EMB: ethambutol;

TB: tuberculosis; Q: flow between central and peripheral compartments; V_c: central compartment volume; C_p: peripheral concentration; C_c: central concentration; V_p: peripheral compartment volume; EC_{50}: delayed concentration resulting in half of the maximal drug effect; E_{max}: the maximal level of drug effect; K_g: bacterial growth rate; $f_{imm(B,t)}$: bacteria- and time-dependent immune inhibition; K_d: bacterial death rate; PopPK: population pharmacokinetics.

from the mean value for each arm reported in each study, and the variability in baseline bacterial burden between individuals used was the baseline variance among all clinical studies. The net growth and death of bacteria without treatment was assumed to be zero (supplementary equation S5). Predictions were reported as the mean±SD of the predicted time course of CFU decline. For drugs where observed data were available, the data were overlaid for visual inspection. Finally, quantitative predictions of commonly reported parameters (change from baseline to day 2 and from day 2 to day 14) were compared to the observed at various dose levels along a line of unity.

Software and statistical method

Pre-clinical and clinical PK-PD modelling was performed in NONMEM (7.4.3) through PsN (4.8.1). For LZD pre-clinical PK modelling, Monolix (5.0.0) was used. Models were developed following numerical and graphical diagnostics, assessing drop in objective function value through the likelihood ratio test and parameter precision, as well as goodness-of-fit plots and visual predictive checks, respectively, in addition to pharmacological relevance. Data transformation and graphical output were performed in R (4.1.3) through the RStudio (2022.02.3) interface using the xpose4 and tidyverse packages.

Results

Large pre-clinical and clinical PK and PD database of 10 TB drugs

We collated a rich longitudinal dataset of mouse PK (plasma concentrations, 1220 data points) and PD data (lung CFU counts, 1550 data points), as well as human population PK models and human PD data (sputum CFU counts) (supplementary table S1). PD experiments were done mostly in mouse infection models infected *via* aerosol with an inoculum size $\geqslant 3.5\ \log_{10}\ CFU{\cdot}mL^{-1}$ and incubation periods of 13–17 days, prior to the start of treatment. Exceptions were EMB and LZD, which had incubation periods of 7 and 5 days, respectively, but had a similar inoculation size of $>3.5\ \log_{10}\ CFU{\cdot}mL^{-1}$, and RPT, which had an incubation period of 41 days, but an inoculation size of $<3.5\ \log_{10}\ CFU{\cdot}mL^{-1}$.

Human PK data were simulated using published models from literature (supplementary table S1 and figure 2c). Human PD data with a total of 287 human sputum CFU datapoints originating from phase 2a trials across 14 different studies ranging from 2 to 14 days were used to validate our phase 2a EBA predictions.

Pre-clinical PK and PK-PD models adequately described mouse data

The final PK and PK-PD model parameter estimates are shown in tables 1 and 2. A two-compartment model with saturated clearance described *via* the Michaelis–Menten equation best described the mouse plasma concentration data for INH, LZD, PMD, PZA and RIF. BDQ, EMB and MXF were best described using two-compartment models with linear elimination; RPT by a one-compartment model with saturated elimination; and DLM by a one-compartment model with linear elimination. Visual predictive checks of the final model for both mouse PK and PK-PD data showed good fits (supplementary figures S1 and S2). The exposure–response relationships for each drug in mouse infection models are summarised in table 1 and supplementary figure S3 and aligned with clinical knowledge of the efficacy of each drug.

Clinical EBA was well predicted by the translational platform

The translational platform predicted clinical EBA in TB patients receiving monotherapy with the 10 drugs, as shown in figure 3. Our predictions overlapped well with the observed data across multiple doses and time points for most of the drugs. BDQ and LZD had slight over-predictions at the later time, and RPT showed activity up to 5 days after a single dose, whereas our model predicted limited declines in CFU.

Agreement between predicted and observed quantitative change in CFU is shown in figure 4 as a correlation plot for EBA at time intervals of 0–2 days and 2–14 days. Most predictions for 0–2 days fell within $0.25\ \log_{10}\ CFU{\cdot}mL^{-1}{\cdot}day^{-1}$ of the observed EBA as indicated by the line of unity and corresponding dotted lines. Predictions for 2–14 days were even closer to observed. Predictions were overall consistent with the observed data in the clinical EBA studies for all 10 drugs, except for RPT, where activity was under-predicted.

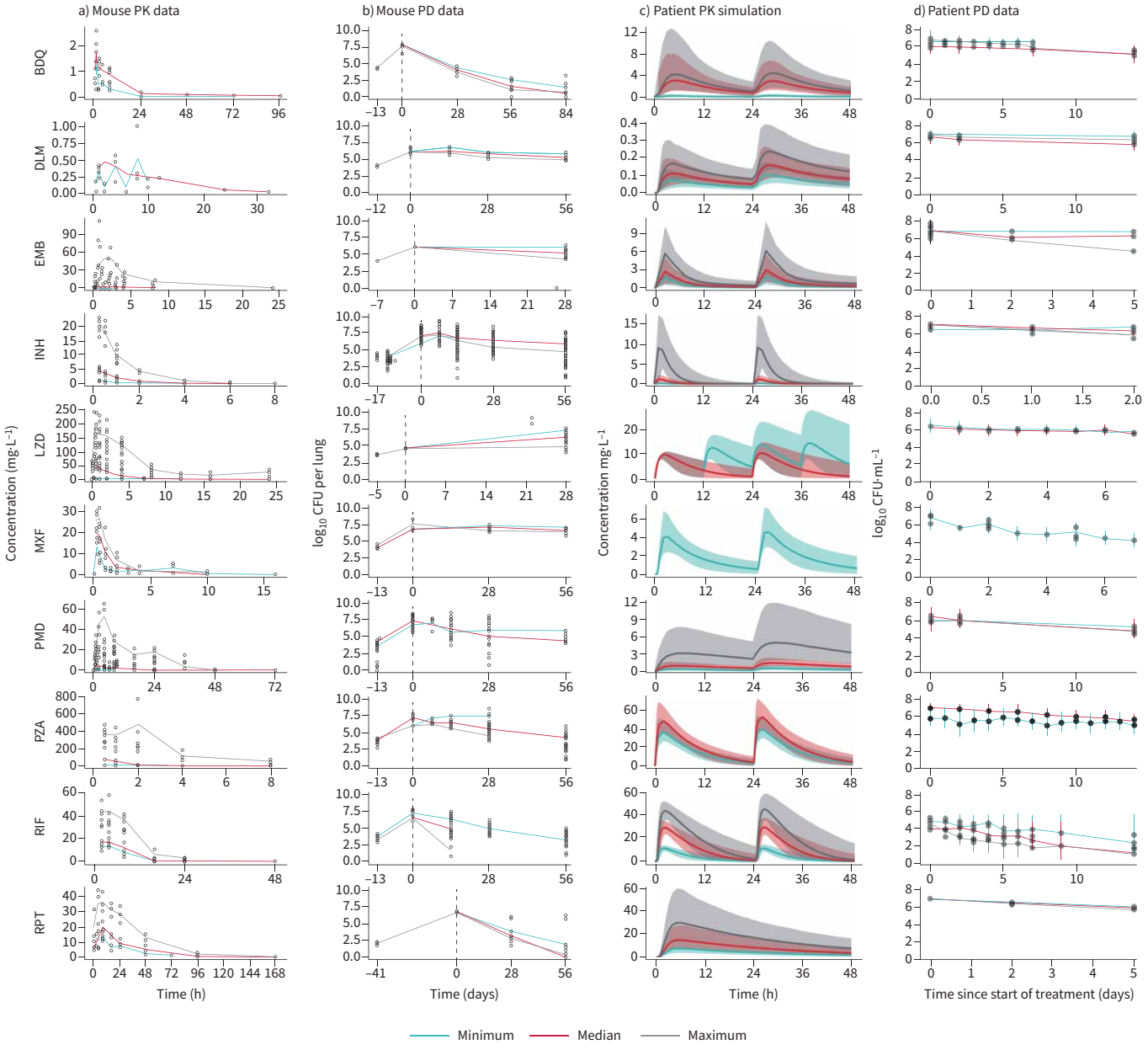

FIGURE 2 A rich dataset of mouse a) pharmacokinetic (PK) and b) pharmacodynamic (PD) and human c) PK and d) PD data for 10 first- and second-line tuberculosis drugs was compiled for model building. Only minimum, median and maximum doses are represented as median lines when multiple doses were present. Data points for all doses are plotted. Information on all doses is present in supplementary table S1. Mouse PK data are presented for the following doses: bedaquiline (BDQ) 12.5, 25 mg·kg^{-1}; delamanid (DLM) 2.5, 3 mg·kg^{-1}; ethambutol (EMB) 10, 30, 1000 mg·kg^{-1}; isoniazid (INH) 1.56, 6.25, 25 mg·kg^{-1}; linezolid (LZD) 5, 100, 500 mg·kg^{-1}; moxifloxacin (MXF) 100, 200, 400 mg·kg^{-1}; pretomanid (PMD) 6, 28.8, 486 mg·kg^{-1}; pyrazinamide (PZA) 7, 100, 900 mg·kg^{-1}; rifampin (RIF) 10, 15, 40 mg·kg^{-1}; rifapentine (RPT) 5, 10, 20 mg·kg^{-1}. All doses were given once daily unless otherwise stated. Mouse PD data are presented for the following doses: BDQ 12.5, 25, 50 mg·kg^{-1}; DLM 3, 10, 100 mg·kg^{-1}; EMB 100, 400, 1600 mg·kg^{-1}; INH 0.1, 6.25, 100 mg·kg^{-1}; LZD 100, 300, 1000 mg·kg^{-1}; MXF 25, 50, 100 mg·kg^{-1}; PMD 50, 100 mg·kg^{-1}; PZA 3, 50, 900 mg·kg^{-1}; RIF 2.5, 40, 640 mg·kg^{-1}; RPT 5, 10, 20 mg·kg^{-1}. All doses were given once daily, 5 days per week, unless otherwise stated. Human PK simulations from validated population PK models presented for the following doses: BDQ 25, 200, 400 mg; DLM 100, 200, 400 mg; EMB 15, 25, 50 mg·kg^{-1}; INH 9, 75, 600 mg; LZD 600 mg once daily, 600 mg twice daily; MXF 400 mg; PMD 50, 200, 1200 mg; PZA 1500, 2000mg; RIF 600, 1350, 1950mg; RPT 300, 600, 1200 mg. All doses were given once daily, unless otherwise stated. Human phase 2a early bactericidal activity study data are presented for the following doses: BDQ 25, 200, 400 mg; DLM 100, 200, 400 mg; EMB 15, 25, 50 mg·kg^{-1}; INH 9, 75, 600 mg; LZD 600 mg once daily, 600 mg twice daily; MXF 400 mg; PMD 50, 200, 1200 mg; PZA 200 mg; RIF 600, 1350, 1950mg; RPT 300, 600, 900, 1200 mg. All doses were given once daily, unless otherwise stated.

TABLE 1 Parameter estimates of final pharmacokinetic (PK) models for 10 tuberculosis drugs in mouse studies

	Structural PK model[#]	PK parameters (RSE)	Protein binding ratio ($f_{u,human/mouse}$)
BDQ	Two-compartment, linear elimination	K_a 3.24 (15.1%) per hour CL 0.0243 (5.9%) L·h^{-1} V_c 0.24 (11.4%) L V_p 0.822 (29.3%) L Q 0.0127 (11.5%) L·h^{-1}	1.0 [38]
DLM	One-compartment, linear elimination	K_a 0.446 (25%) per hour CL 0.0092 (8%) L·h^{-1} V_c 0.0747 (1%) L $F_{3mg/kg}$ 0.758 (5%)	1.0 [39]
EMB [7]	Two-compartment, linear elimination	CL 0.0512 (5.9%) L·h^{-1} V_c 0.0436 (12.8%) L V_p 0.0982 (7.6%) L K_a 0.869 (9.9%) per hour Q 0.0352 (13.5%) L·h^{-1} F 0.64 (6.7%) A_{lag} 0.0577 (11.1) h	1.0
INH	Two-compartment, saturated elimination	CL_{int} 31.5 (8.1%) mL·h^{-1} K_m 13.1 (23.2%) µg·mL^{-1} K_a 7.89 (89.4%) per hour V_c 18.6 (45.0%) mL Q 13.3 (97.7%) mL·h^{-1} V_p 9.77 (66.4%) mL	1.455 [40, 41]
LZD	Two-compartment, saturated elimination	K_a 10 per hour (fixed) CL_{int} 0.0526 L·h^{-1} V_c 0.0178 L V_p 0.00836 L Q 0.00175 L·h^{-1} K_m 8.03 mg·L^{-1}	0.986 [13, 42]
MXF	Two-compartment, linear elimination	K_a 0.0723 (10%) per hour Q 0.1269 (20%) L·h^{-1} V_c 0.09423 (7%) L V_p 0.3504 (25%) L CL 0.119 (12%) L·h^{-1}	0.797 [43]
PMD	Two-compartment, saturated elimination and bioavailability	K_a 2.94 (31%) per hour CL_{int} 0.0392 (9%) L·h^{-1} V_c 0.158 (7%) L V_p 0.00568 (71%) L Q 0.00009 (18%) L·h^{-1} K_m 2.74 (24%) mg·L^{-1} F_{dif} 1 (fixed) FD_{50} 363 mg·kg^{-1} γ 1 (fixed)	0.71 [40, 44]
PZA	Two-compartment, saturated elimination and bioavailability	CL_{int} 14.4 (12%) mL·h^{-1} K_m 82.9 (61%) µg·mL^{-1} K_a 100 per hour (fixed) V_c 13.3 (49%) mL Q 3.11 (19%) mL·h^{-1} V_p 10.9 (37%) mL $F_{7mg/kg}$ (fixed) FD_{50} 18.2 (23%) mg·kg^{-1} F_{dif} 0.574 (34%)	0.925 [12]
RIF	Two-compartment, saturated elimination and bioavailability	V_{max} 15.2 (6%) µg·h^{-1} K_m 1.16 (20%) µg·mL^{-1} K_a 0.272 (10%) per hour V_1 3.39 (12%) mL Q 0.725 (6%) mL·h^{-1} V_2 27.4 (39%) mL $F_{10mg/kg}$ (fixed) $F_{15mg/kg}$ 0.743 (0%) $F_{20mg/kg}$ 0.845 (1%) $F_{40mg/kg}$ 0.493 (2%)	4.545 [41, 45]

Continued

TABLE 1 Continued

	Structural PK model[#]	PK parameters (RSE)	Protein binding ratio ($f_{u,human/mouse}$)
RPT	One-compartment, saturated elimination	K_a 0.894 (31%) per hour V 0.0139 (6%) L K_m 75.8 (31%) μg·mL^{-1} V_{max} 0.0333 (24%) μg·h^{-1}	0.422 [46, 47]

RSE: relative standard error; BDQ: bedaquiline; DLM: delamanid; EMB: ethambutol; INH: isoniazid; LZD: linezolid; MXF: moxifloxacin; PMD: pretomanid; PZA: pyrazinamide; RIF: rifampin; RPT: rifapentine; K_a: rate of absorption; CL: linear clearance; V_c: central compartment volume; V_p: peripheral compartment volume; Q: flow between central and peripheral compartments; K_m: concentration that produces half the maximum rate of elimination; V_{max}: maximum rate of elimination; CL_{int}: intrinsic clearance describing saturated elimination; F: the extent of drug absorbed from oral dosing compartment into systemic compartment; F_{dif}: the maximum difference in bioavailability from 100% (bound between 0% and 100%); FD_{50}: the dose achieving half maximal reduction in bioavailability; A_{lag}: absorption lag time; γ: the steepness of the relationship between the (delayed) plasma concentration and drug effect. [#]: complete equations for PK models are found in supplementary equations S6–S12; one-compartment model indicates that distribution and elimination phases of the drug were almost instantaneous and can be described by a single central compartment; two-compartment model indicates that distribution and elimination phases of the drug were distinct and can be described by a central compartment and a peripheral compartment; linear elimination indicates that elimination pathways were not saturated with higher doses for the tested dose range; saturated elimination indicates elimination plateaus after a certain dose (this relationship can be described by a Michaelis–Menten equation using K_m and V_{max}).

Discussion

We established a mouse-to-human translational platform by integrating a bacterial dynamics model, mouse PK-PD relationships, clinical PK models and species-specific drug plasma protein binding, and validated the platform with clinical EBA data (figure 1). The changes in sputum CFU counts over the first 2 days and from day 2 to day 14 in TB patients receiving monotherapy with each of 10 TB drugs in 14 clinical EBA studies spanning more than four decades were predicted successfully (figures 3 and 4). Compared to the participants enrolled in more recent EBA studies (2007 to 2015) [17–23] at the same site, the participants enrolled between 1992 and 2005 [24–28] had more severe disease and therefore higher baseline CFU counts in their sputum samples (mean baseline 6.9 $\log_{10}$ CFU·mL^{-1}). However, the predictive accuracy of our model was robust despite this large variation in baseline bacterial burden. For example, RIF had a good overlap of predicted and observed EBA (figure 3) despite the study being conducted in 2015 with the lowest median baseline of 4.58 $\log_{10}$ CFU·mL^{-1} [18].

A key component to our model accuracy was the addition of the bacterial dynamics model. Mouse and human immune activation against TB infection differ significantly; therefore, the underlying baseline of bacterial dynamics will differ. Subtracting the mouse immune effect on bacterial decline more accurately estimates the drug contribution to CFU decline. Without such consideration, the clinical CFU decline was over-predicted (supplementary figure S4). Despite inherent differences between species in terms of drug pharmacokinetics, sampling (whole lung homogenate *versus* sputum), and infecting bacterial strain, the relationship between drug effect on bacteria and the concentration to achieve the effect appear, based on this analysis, to be portable between mice and patients. In addition, although the mouse strain used in the studies (BALB/c) models intracellular bacteria, but not extracellular bacteria in caseous lesions [29], the PK-PD relationships observed in this model, when derived in comparison to the baseline bacterial dynamics, appear to accurately reflect those observed in EBA studies. Other approaches or more information may be needed to fully account for drug exposures at the site of infection in cavities or other caseous lesions or any PK-PD relationships unique to those microenvironments.

Murine TB models are routinely and often exclusively used as *in vivo* efficacy models in pre-clinical TB drug development [1]. As the inoculum size and incubation period for bacterial infection in the lung prior to treatment can affect drug response [8], we standardised our inclusion criteria to experiments using the most common design with the incubation duration of 13–17 days and inoculum size to $\geqslant$3.5 $\log_{10}$ CFU·mL^{-1}. Incubation durations outside this range were considered only when data were otherwise not available, which was the case for EMB, LZD and RPT.

Clinical EBA studies are the only acceptable way to evaluate a drug as monotherapy in TB patients despite their limitations in predicting long-term efficacy. In addition to detecting the presence of an EBA response,

TABLE 2 Parameter estimates of final pharmacokinetic (PK)-pharmacodynamic (PD) models for 10 tuberculosis drugs in mouse studies

	PK-PD model	PK-PD model parameters	Mouse infection model type
BDQ	Direct E_{max} function	E_{max} 0.515 (1%) per day EC_{50} 0.228 (5%) mg·L^{-1}	Subacute
DLM	Delayed E_{max} function	E_{max} 0.248 (23%) per day EC_{50} 1.02 (63%) mg·L^{-1} K_{delay} 91.4 (0.2%) per day	Subacute
EMB	Direct E_{max} function	E_{max} 0.527 (2%) per day EC_{50} 0.150 (17%) mg·L^{-1}	Acute
INH	Delayed E_{max} function	E_{max} 0.901 (7.5%) per day EC_{50} 0.00404 (55%) mg·L^{-1} K_{delay} 7.51 (20%) per day	Subacute
LZD	Delayed sigmoidal function	E_{max} 1 per day (fixed) EC_{50} 2.77 (1%) mg·L^{-1} γ 0.21 (3%) K_{delay} 6.75 (0%) per day	Acute
MXF	Delayed E_{max} function	E_{max} 0.553 (10%) per day EC_{50} 0.0000586 (44%) mg·L^{-1} K_{delay} 0.0000708 (0.07%) per day	Subacute
PMD	Direct sigmoidal function	E_{max} 0.429 (0.1%) per day EC_{50} 3.46 (0.3%) mg·L^{-1} γ 0.375 (1%) per day	Subacute
PZA	Delayed E_{max} function	E_{max} 0.34 (10%) per day EC_{50} (AUC) 13.6 (42%) mg·day·L^{-1} K_{delay} 0.797 (0.2%) per day	Subacute
RIF	Delayed sigmoidal function	E_{max} 0.678 (16%) per day EC_{50} 1.92 (39%) mg·L^{-1} γ 1.38 (24%) K_{delay} 1.34 (79%) per day	Subacute
RPT	Direct sigmoidal function	E_{max} 0.299 (1%) per day EC_{50} 6.02 (0%) mg·L^{-1} γ 2.36 (7%)	Chronic

BDQ: bedaquiline; DLM: delamanid; EMB: ethambutol; INH: isoniazid; LZD: linezolid; MXF: moxifloxacin; PMD: pretomanid; PZA: pyrazinamide; RIF: rifampin; RPT: rifapentine; E_{max}: the maximal level of drug effect; EC_{50}: the delayed concentration that results in half of the maximal drug effect; K_{delay}: the delay rate of the plasma concentration associated with drug effect; γ: the steepness of the relationship between the (delayed) plasma concentration and drug effect. Equations are presented as supplementary equations S3 and S4.

the trial can inform on the dose–response curve (*e.g.* INH and RIF), which could be used in dose selection for future trials [18, 30, 31]. We have shown here that our translational platform can adequately predict these EBAs for different doses. With limited resources, this costly clinical study can be designed more efficiently or avoided altogether by using our approach to predict a reliable result regarding clinical dose–response effects, and to provide useful information about dose and/or drug candidate selection for further clinical development. This scenario is well exemplified by the nitroimidazole, PMD. PMD has a dose response at doses up to 192 mg·kg^{-1} in mice, which, following the conventional allometric scaling method, approximates 1500 mg in humans. However, such translation is problematic, as the clinical observations from two human EBA trials demonstrated no dose response above 200 mg in human EBA. Using our translational platform, we found that the drug effect of PMD reaches plateau after 200 mg, which is consistent with clinical observations (supplementary figure S3). Therefore, our translational platform could serve as a powerful tool for, but not limited to, better dose selection for clinical trials design. By better informing dose selection, the translational modelling platform may reduce the time and effort spent in early clinical development, and therefore, accelerate progress to trials that are more informative of long-term outcomes.

Phase 2a trials also gather information on initial safety and tolerability of compounds of interest, which our translational framework is not designed to predict. However, when anti-TB drug development progresses directly to regimen efficacy studies, these safety data can have already been captured during phase 1 healthy volunteer monotherapy studies, especially the multiple ascending dose study which is a dose-ranging study for up to 4 weeks. The trial population of healthy volunteers is different from the

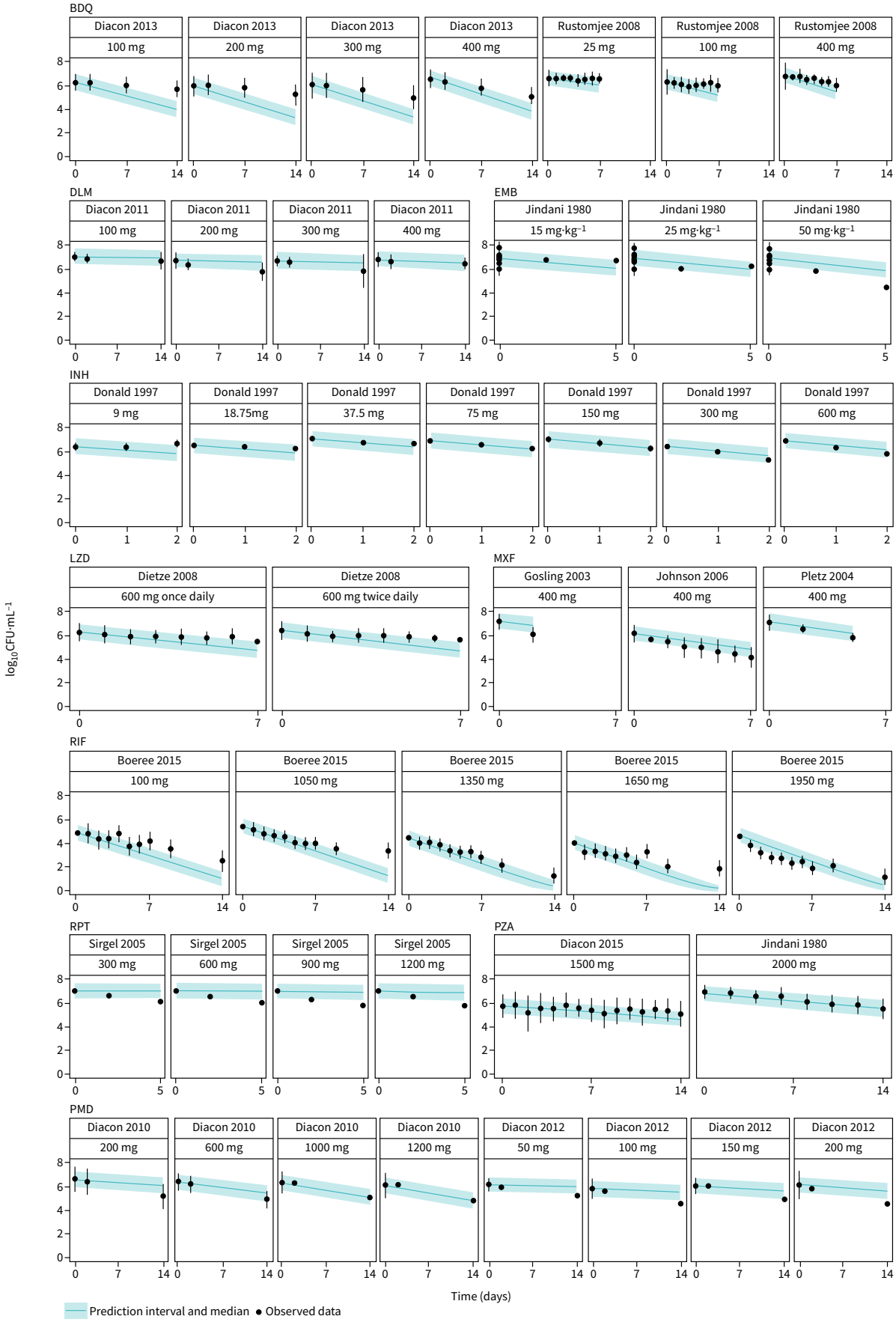
BDQ
Diacon 2013 100 mg
Diacon 2013 200 mg
Diacon 2013 300 mg
Diacon 2013 400 mg
Rustomjee 2008 25 mg
Rustomjee 2008 100 mg
Rustomjee 2008 400 mg
DLM
Diacon 2011 100 mg
Diacon 2011 200 mg
Diacon 2011 300 mg
Diacon 2011 400 mg
EMB
Jindani 1980 15 mg·kg⁻¹
Jindani 1980 25 mg·kg⁻¹
Jindani 1980 50 mg·kg⁻¹
INH
Donald 1997 9 mg
Donald 1997 18.75mg
Donald 1997 37.5 mg
Donald 1997 75 mg
Donald 1997 150 mg
Donald 1997 300 mg
Donald 1997 600 mg
LZD
Dietze 2008 600 mg once daily
Dietze 2008 600 mg twice daily
MXF
Gosling 2003 400 mg
Johnson 2006 400 mg
Pletz 2004 400 mg
RIF
Boeree 2015 100 mg
Boeree 2015 1050 mg
Boeree 2015 1350 mg
Boeree 2015 1650 mg
Boeree 2015 1950 mg
RPT
Sirgel 2005 300 mg
Sirgel 2005 600 mg
Sirgel 2005 900 mg
Sirgel 2005 1200 mg
PZA
Diacon 2015 1500 mg
Jindani 1980 2000 mg
PMD
Diacon 2010 200 mg
Diacon 2010 600 mg
Diacon 2010 1000 mg
Diacon 2010 1200 mg
Diacon 2012 50 mg
Diacon 2012 100 mg
Diacon 2012 150 mg
Diacon 2012 200 mg
log10CFU·mL⁻¹
Time (days)
Prediction interval and median
Observed data

FIGURE 3 Translational (mouse to human) pharmacokinetic (PK)-pharmacodynamic (PD) model predicts clinical early bactericidal activity (EBA) trial results well. Median (95% CI) of 1000 simulations from the translational model overlap with observed EBA data from clinical trials. BDQ: bedaquiline; DLM: delamanid; EMB: ethambutol; INH: isoniazid; LZD: linezolid; MXF: moxifloxacin; RIF: rifampin; RPT: rifapentine; PZA: pyrazinamide; PMD: pretomanid.

patient population, but safety signals are more pronounced in this healthy population that is more sensitive to adverse events and less burdened by other symptoms. For example, treatment of healthy volunteers with rifapentine resulted in safety signals, but has been proven safe in patients with TB [32]. Furthermore, we can also get guidance on the optimal efficacious dose *versus* the safety range using the dose–response curve by overlaying both exposures (supplementary figure S3). All our studied drugs have been approved previously and are used clinically. Having all clinical dose exposures lower than safety limits were thus unsurprising and reassuring. Such dose–response curves as visualisation would be helpful for determining the dose of new TB drugs too, as they provide a measure of both efficacy and safety.

Of the clinical EBA studies included in our analysis, the RPT EBA trial was the only one in which EBA was assessed for multiple days after a single dose. Our human population PK model indicated that RPT was mostly cleared from the body 2 days after a single dose, but the trial results indicated that RPT was still exerting an effect on bacterial load between 2 and 5 days post-dose. It is possible that RPT has a post-antibiotic effect that was not sufficiently captured by the model. The model over-predicted the EBA of BDQ. However, in the model, the active metabolite, BDQ-M2, was not considered. In mice, M2 is estimated to contribute ~50% of the drug effect. One possible reason for the over-prediction are the parent-to-metabolite ratios between species that differ, where mice have higher M2-to-BDQ ratios than humans [33]. Future studies can account for these differences.

Our translational framework has been developed to predict clinical EBA in the typical adult patient population participating in EBA trials. Heterogeneity in the patient population is an important consideration in drug development and individualised medicine [34]. This is both from the perspective of representing patients in easy- or hard-to-treat phenotypes, as we have observed in our clinical projects as a result from different risk factors (baseline bacterial burden, disease phenotype such as cavitation, gender, comorbidities or co-medications), as well as from a diversity perspective to study pharmacology in under-represented individuals [35, 36]. Certain risk factors such as baseline bacterial burden are easily implementable in our clinical simulations, as well as, for example, the influence of comorbidities or

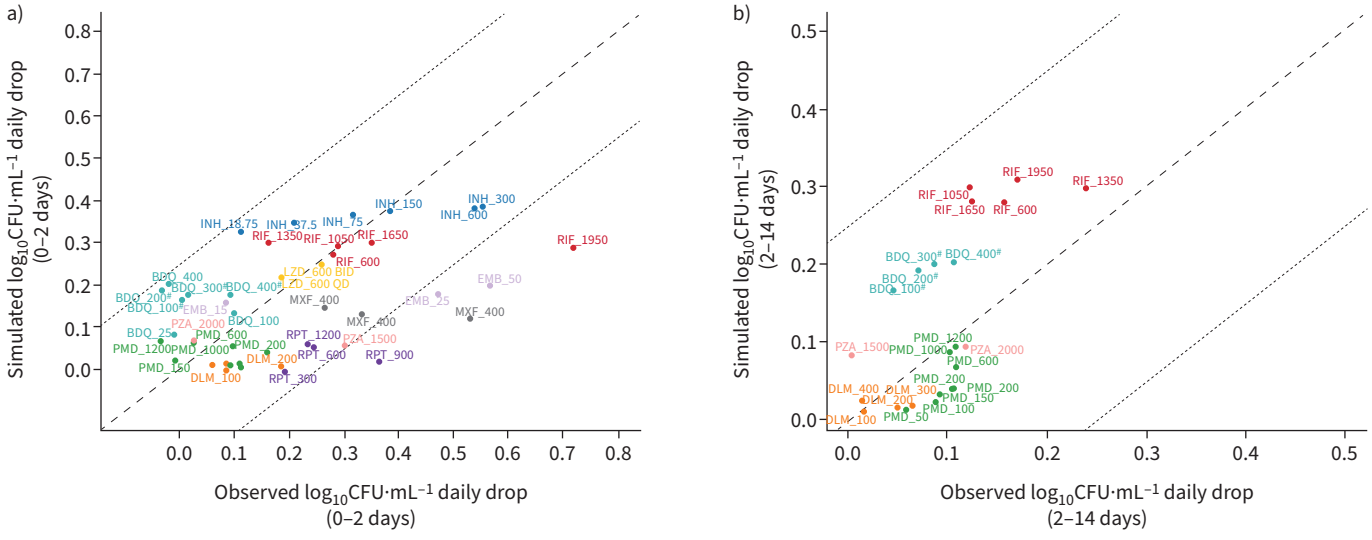

FIGURE 4 Model-based prediction of daily change in log_{10} CFU·mL^{-1} correlates well with clinically observed daily change in log_{10} CFU·mL^{-1} for 10 tuberculosis drugs at multiple dose levels of monotherapy between a) days 0–2 and b) days 2–14. For some drugs, day 14 data were not available. Data are presented as line of unity±0.25. BDQ: bedaquiline; DLM: delamanid; EMB: ethambutol; INH: isoniazid; LZD: linezolid; MXF: moxifloxacin; PMD: pretomanid; PZA: pyrazinamide; RIF: rifampin; RPT: rifapentine. #: regimen contained a loading dose.

co-medications on the pharmacokinetics. However, pre-clinical (mouse) models are traditionally more homogeneous to reduce noise in the data and be more sensitive to detect pharmacological signals. At the same time, the EBA trials with relatively small sample sizes (<15 per arm) will also not reflect clinical heterogeneity, and risk factors other than those described have limited relevance for the prediction of the EBA (*e.g.* cavitation). Similar considerations are applicable to the prediction of EBA in children. Throughout their development, infants and children show changes in their pharmacology that are well established and can be incorporated in our quantitative model-based framework. Pharmacodynamically, the bacterial dynamics and the disease phenotype differences can be modelled based on different animal disease models. Children with TB aged <1 year have limited immunity, which can be approximated through the immunocompromised athymic (nude) mouse model, while dose for those aged >1 year without lesion phenotypes can be approximated through the BALB/c mouse model. One limitation of these pre-clinical models is their reliance of bacterial load measurement, which is complicated in the paediatric population in the context of sputum collection. Alternative models are being developed which are part of future collaborative work in our group. Pharmacokinetically, the development of the metabolic pathways responsible for the elimination of anti-TB drugs can be incorporated through the use of maturation functions. As a result, paediatric dosing can be projected that will reach similar exposure as in adults given a chosen dose, based on the understanding of the maturation of the relevant elimination pathways and the adult pharmacokinetics.

Building on our translational framework, we aim to predict the efficacy of combination regimens of TB drugs in long-term TB clinical outcomes for phase 2b and 3 from pre-clinical mouse data. Being able to better understand the time to stable culture conversion and relapse 6 months post-treatment will better help us prioritise sterilising regimens. We hope to achieve this by including the characterisation of PK-PD relationships in combination regimens by accounting for PK-PD drug–drug interactions, as well as characterising lesion-specific PK-PD relationships. Technically, the bacterial dynamic parameters of the translational tool will be re-evaluated and possibly updated through Bayesian methods based on untreated control data of ongoing experiments with novel anti-TB drugs, benefiting from a larger data collection while keeping the structure of the translational tool. Clinical TB disease (*e.g.* caseation necrosis and cavitation) will be represented in the translational platform to include infection and efficacy data in animal models of TB with more human-like necrotic lesions, such as C3HeB/FeJ mice and New Zealand white rabbits [37]. This will allow us to have a comprehensive platform that informs us not only of monotherapy EBA, but also combination drug regimen efficacy in providing a stable cure and prevention of long-term unfavourable outcomes.

In summary, we established a foundation for translating the results from mouse efficacy models to clinical EBA studies through establishing quantitative relationships involving mouse PK and PD models, as well as drug dose response *in vivo*. In the future, our platform will be expanded to include combination regimens and longer durations of treatment by accounting for PK-PD drug–drug interactions and necrotic lesion penetration. This platform is an innovation to accelerate TB drug development and a good example of model-informed drug discovery and development.

Acknowledgements: We acknowledge TB Alliance for support and generously sharing the in-house data of anti-TB drugs linezolid and pretomanid.

Author contributions: The manuscript was written by J.P. Ernest, J.J.N. Goh, N. Strydom, Q. Wang, R.C. van Wijk and N. Zhang and commented on by all authors. J.P. Ernest, J.J.N. Goh, N. Strydom, Q. Wang, R.C. van Wijk and N. Zhang contributed to data collection, model development, data and model management, and code review. Contributions to data collection and model development were as follows. J.P. Ernest: BDQ and RPT; J.J.N. Goh: EMB; N. Strydom: LZD; Q. Wang: DLM, PMD and MXF; N. Zhang: PZA, RIF and INH. J.J.N. Goh and R.C. van Wijk revised the manuscript, including generation of figures and tables. J.P. Ernest and R.C. van Wijk carried out code review for all drugs. A. Deitchman worked on data collection, human PK model development, simulation, and preliminary model development. E. Nuermberger provided pre-clinical data used in our current study, provided substantial scientific context, and edited the manuscript. R.M. Savic supervised the whole research.

Conflict of interest: R.M. Savic and E. Nuermberger report support for the present work from TB Alliance and National Institutes of Health. In addition, E. Nuermberger also reports advisory board participation with Janssen, outside the submitted work. The remaining authors have no potential conflicts of interest to disclose.

Support statement: This work was supported by NIH grant R01AI-111992. Funding information for this article has been deposited with the Crossref Funder Registry.

References

1 Nuermberger EL. Preclinical efficacy testing of new drug candidates. *Microbiol Spectr* 2017; 5: 10.1128/microbiolspec.TBTB2-0034-2017.
2 Jindani A, Aber VR, Edwards EA, *et al.* The early bactericidal activity of drugs in patients with pulmonary tuberculosis. *Am Rev Respir Dis* 1980; 121: 939–949.
3 Van Norman GA. Phase II trials in drug development and adaptive trial design. *JACC Basic Transl Sci* 2019; 4: 428–437.
4 US Department of Health and Human Services Food and Drug Administration Center for Drug Evaluation and Research (CDER). Pulmonary Tuberculosis: Developing Drugs for Treatment Guidance for Industry. Draft Guidance. 2022. www.fda.gov/media/87194/download
5 Danhof M, de Lange ECM, Della Pasqua OE, *et al.* Mechanism-based pharmacokinetic-pharmacodynamic (PK-PD) modeling in translational drug research. *Trends Pharmacol Sci* 2008; 29: 186–191.
6 Sasahara K, Shimokawa Y, Hirao Y, *et al.* Pharmacokinetics and metabolism of delamanid, a novel anti-tuberculosis drug, in animals and humans: importance of albumin metabolism *in vivo*. *Drug Metab Dispos* 2015; 43: 1267–1276.
7 Chen C, Ortega F, Alameda L, *et al.* Population pharmacokinetics, optimised design and sample size determination for rifampicin, isoniazid, ethambutol and pyrazinamide in the mouse. *Eur J Pharm Sci* 2016; 93: 319–333.
8 Zhang N, Strydom N, Tyagi S, *et al.* Mechanistic modeling of *Mycobacterium tuberculosis* infection in murine models for drug and vaccine efficacy studies. *Antimicrob Agents Chemother* 2020; 64: e01727-19.
9 US Department of Health and Human Services Food and Drug Administration Center for Drug Evaluation and Research (CDER). Guidance for Industry: Estimating the Maximum Safe Starting Dose in Initial Clinical Trials for Therapeutics in Adult Healthy Volunteers. 2005. www.fda.gov/media/72309/download
10 Svensson EM, Dosne A-G, Karlsson MO. Population pharmacokinetics of bedaquiline and metabolite M2 in patients with drug-resistant tuberculosis: the effect of time-varying weight and albumin. *CPT Pharmacometrics Syst Pharmacol* 2016; 5: 682–691.
11 Patterson S, Wyllie S, Norval S, *et al.* The anti-tubercular drug delamanid as a potential oral treatment for visceral leishmaniasis. *Elife* 2016; 5: e09744.
12 Alghamdi WA, Al-Shaer MH, Peloquin CA. Protein binding of first-line antituberculosis drugs. *Antimicrob Agents Chemother* 2018; 62: e00641-18.
13 Dryden MS. Linezolid pharmacokinetics and pharmacodynamics in clinical treatment. *J Antimicrob Chemother* 2011; 66: iv7–iv15.
14 Dorn C, Nowak H, Weidemann C, *et al.* Decreased protein binding of moxifloxacin in patients with sepsis? *GMS Infect Dis* 2017; 5: Doc03.
15 Committee for Medicinal Products for Human Use (CHMP). Assessment Report: Pretomanid FGK International Non-Proprietary Name: Pretomanid. 2020. www.ema.europa.eu/en/documents/assessment-report/pretomanid-fgk-epar-public-assessment-report_en.pdf
16 Egelund EF, Weiner M, Singh RP, *et al.* Protein binding of rifapentine and its 25-desacetyl metabolite in patients with pulmonary tuberculosis. *Antimicrob Agents Chemother* 2014; 58: 4904–4910.
17 Diacon AH, Dawson R, du Bois J, *et al.* Phase II dose-ranging trial of the early bactericidal activity of PA-824. *Antimicrob Agents Chemother* 2012; 56: 3027–3031.
18 Boeree MJ, Diacon AH, Dawson R, *et al.* A dose-ranging trial to optimize the dose of rifampin in the treatment of tuberculosis. *Am J Respir Crit Care Med* 2015; 191: 1058–1065.
19 Diacon AH, Dawson R, Hanekom M, *et al.* Early bactericidal activity of delamanid (OPC-67683) in smear-positive pulmonary tuberculosis patients. *Int J Tuberc Lung Dis* 2011; 15: 949–954.
20 Rustomjee R, Diacon AH, Allen J, *et al.* Early bactericidal activity and pharmacokinetics of the diarylquinoline TMC207 in treatment of pulmonary tuberculosis. *Antimicrob Agents Chemother* 2008; 52: 2831–2835.
21 Diacon AH, Dawson R, Von Groote-Bidlingmaier F, *et al.* Randomized dose-ranging study of the 14-day early bactericidal activity of bedaquiline (TMC207) in patients with sputum microscopy smear-positive pulmonary tuberculosis. *Antimicrob Agents Chemother* 2013; 57: 2199–2203.
22 Dietze R, Hadad DJ, McGee B, *et al.* Early and extended early bactericidal activity of linezolid in pulmonary tuberculosis. *Am J Respir Crit Care Med* 2008; 178: 1180–1185.
23 Diacon AH, Dawson R, von Groote-Bidlingmaier F, *et al.* Bactericidal activity of pyrazinamide and clofazimine alone and in combinations with pretomanid and bedaquiline. *Am J Respir Crit Care Med* 2015; 191: 943–953.
24 Donald PR, Sirgel FA, Botha FJ, *et al.* The early bactericidal activity of isoniazid related to its dose size in pulmonary tuberculosis. *Am J Respir Crit Care Med* 1997; 156: 895–900.
25 Gosling RD, Uiso LO, Sam NE, *et al.* The bactericidal activity of moxifloxacin in patients with pulmonary tuberculosis. *Am J Respir Crit Care Med* 2003; 168: 1342–1345.
26 Johnson JL, Hadad DJ, Boom WH, *et al.* Early and extended early bactericidal activity of levofloxacin, gatifloxacin and moxifloxacin in pulmonary tuberculosis. *Int J Tuberc Lung Dis* 2006; 10: 605–612.

27 Pletz MWR, De Roux A, Roth A, *et al.* Early bactericidal activity of moxifloxacin in treatment of pulmonary tuberculosis: a prospective, randomized study. *Antimicrob Agents Chemother* 2004; 48: 780–782.
28 Sirgel FA, Fourie PB, Donald PR, *et al.* The early bactericidal activities of rifampin and rifapentine in pulmonary tuberculosis. *Am J Respir Crit Care Med* 2005; 172: 128–135.
29 Kramnik I, Beamer G. Mouse models of human TB pathology: roles in the analysis of necrosis and the development of host-directed therapies. *Semin Immunopathol* 2016; 38: 221–237.
30 Diacon AH, Pym A, Grobusch MP, *et al.* Multidrug-resistant tuberculosis and culture conversion with bedaquiline. *N Engl J Med* 2014; 371: 723–732.
31 Donald PR, Diacon AH. The early bactericidal activity of anti-tuberculosis drugs: a literature review. *Tuberculosis* 2008; 88: Suppl. 1, S75–S83.
32 Dooley KE, Bliven-Sizemore EE, Weiner M, *et al.* Safety and pharmacokinetics of escalating daily doses of the antituberculosis drug rifapentine in healthy volunteers. *Clin Pharmacol Ther* 2012; 91: 881–888.
33 Ngwalero P, Brust JCM, van Beek SW, *et al.* Relationship between plasma and intracellular concentrations of bedaquiline and its M2 metabolite in South African patients with rifampin-resistant tuberculosis. *Antimicrob Agents Chemother* 2021; 65: e0239920.
34 Brown K, Etrouth S, Jayachandran P, *et al.* Diversity in clinical pharmacology: a call to action. *Clin Pharmacol Ther* 2023; 113: 483–485.
35 Imperial MZ, Nahid P, Phillips PPJ, *et al.* A patient-level pooled analysis of treatment-shortening regimens for drug-susceptible pulmonary tuberculosis. *Nat Med* 2018; 24: 1708–1715.
36 Imperial MZ, Phillips PPJ, Nahid P, *et al.* Precision-enhancing risk stratification tools for selecting optimal treatment durations in tuberculosis clinical trials. *Am J Respir Crit Care Med* 2021; 204: 1086–1096.
37 Ernest JP, Strydom N, Wang Q, *et al.* Development of new tuberculosis drugs: translation to regimen composition for drug-sensitive and multidrug-resistant tuberculosis. *Annu Rev Pharmacol Toxicol* 2021; 61: 495–516.
38 Janssen Therapeutics. Highlights of Prescribing Information: Sirturo® (Bedaquiline) Tablets, For Oral Use. www.janssenlabels.com/package-insert/product-monograph/prescribing-information/SIRTURO-pi.pdf. Date last updated: September 2021.
39 Shimokawa Y, Sasahara K, Koyama N, *et al.* Metabolic mechanism of delamanid, a new anti-tuberculosis drug, in human plasma. *Drug Metab Dispos* 2015; 43: 1277–1283.
40 Jayaram R, Shandil RK, Gaonkar S, *et al.* Isoniazid pharmacokinetics-pharmacodynamics in an aerosol infection model of tuberculosis. *Antimicrob Agents Chemother* 2004; 48: 2951–2957.
41 Woo J, Cheung W, Chan R, *et al. In vitro* protein binding characteristics of isoniazid, rifampicin, and pyrazinamide to whole plasma, albumin, and α-1-acid glycoprotein. *Clin Biochem* 1996; 29: 175–177.
42 Lepak AJ, Marchillo K, Pichereau S, *et al.* Comparative pharmacodynamics of the new oxazolidinone tedizolid phosphate and linezolid in a neutropenic murine *Staphylococcus aureus* pneumonia model. *Antimicrob Agents Chemother* 2012; 56: 5916–5922.
43 Siefert HM, Domdey-Bette A, Henninger K, *et al.* Pharmacokinetics of the 8-methoxyquinolone, moxifloxacin: a comparison in humans and other mammalian species. *J Antimicrob Chemother* 1999; 43: Suppl. B, 69–76.
44 Rakesh, Bruhn DF, Scherman MS, *et al.* Synthesis and evaluation of pretomanid (PA-824) oxazolidinone hybrids. *Bioorg Med Chem Lett* 2016; 26: 388–391.
45 de Steenwinkel JEM, Aarnoutse RE, de Knegt GJ, *et al.* Optimization of the rifampin dosage to improve the therapeutic efficacy in tuberculosis treatment using a murine model. *Am J Respir Crit Care Med* 2013; 187: 1127–1134.
46 Sanofi. Highlights of Prescribing Information: Priftin (Rifapentine) Tablets, for Oral Use. 2020. https://products.sanofi.us/priftin/priftin.pdf. Date last updated: July 2021.
47 Assandri A, Ratti B, Cristina T. Pharmacokinetics of rifapentine, a new long lasting rifamycin, in the rat, the mouse and the rabbit. *J Antibiot* 1984; 37: 1066–1075.